

Shadow Detection Algorithm and its Performance Evaluation

Ashwini V. Khekade¹

¹M.Tech Student

¹Department of Information Technology

¹Yeshwantrao Chavan College of Engineering Nagpur, India

Abstract— In color aerial images, shadows appearing in images may cause false color tones, loss of feature information, and shape distortion of objects, which affects further image processing tasks. Hence, shadow detection is one of the challenging tasks in image processing. In this work simple and efficient chromaticity-based approach for shadow detection is applied on color aerial images. The technique is applied in various color spaces including HSI, HSV, HCV, YIQ and YCbCr models that decouple luminance and chromaticity. In our work the existing technique is extended, to further enhance the shadow detection results using proposed post processing methods. The experimental results shows effectiveness of our approach in comparison with the results obtained using the original approach without post-processing. Performance evaluation metrics one used to evaluate the performance of the proposed method.

Key words: RGB Color Model, Various Color Models, Color Aerial Images, Shadows, Shadow Detection

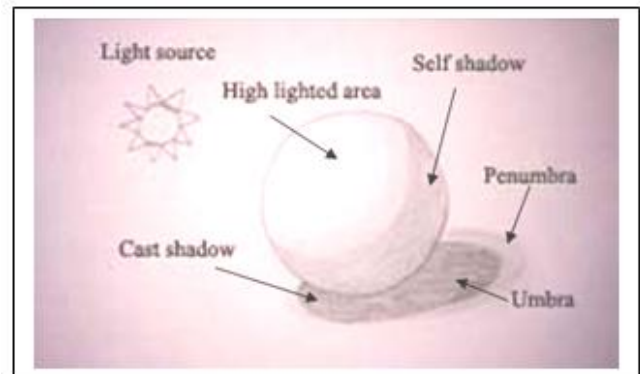


Fig. 1: Shadow Types

I. INTRODUCTION

Shadows in images are significant and may create some problems in image processing and pattern recognition tasks. Shadows in urban imagery are usually cast by elevated objects such as buildings, bridges, towers, etc. when they are illuminated by the sunlight at the time of exposure. Shadows can provide additional structural and morphological signs of its casting body and the position of the light source [1]-[3]. The shadow and non shadow regions are created only when the light energy is fallen on the object. In this paper, chromaticity-based approach is used to detect shadows in color aerial images as suggested in [1]. The approach escapades the properties of shadows in luminance and chromaticity components and is applied in several color spaces, including Red, Green, Blue (RGB), including HIS, HSV, HCV, YIQ, and YCbCr models.

A. Shadow and its Types:

A shadow is an area where light from a light source is blocked by an object. It occupies all of the space behind an impenetrable object with light in front of it. Simply, shadow is made when an object blocks light [5]-[7]. In general, shadows can be categorized into two types such as Cast shadow and Self shadow as shown in fig. 1[8]. A cast shadow is projected by the object toward of the light source; a self shadow is the part of the object that is not illuminated by direct light. The part of a cast shadow where direct light is completely space acquired by its object is called umbra; the part where direct light is partially blocked is called penumbra. The causes of shadow can be grouped into three categories: 1) Shadow by urban materials such as building and trees. 2) Shadow by mountain (topographic shadow). 3) Cloud shadows [9].

B. Color Models:

Basically, the color that human beings perceive in an object is determined by the quality of a chromatic light source in three quantities: radiance, luminance, and brightness [1], [10].

C. RGB Color Model:

In color aerial images, color tone is a powerful descriptor that simplifies and dominates feature identification and extraction in visual interpretation applications. Basically, the color that human beings perceive in an object is determined by the quality of a chromatic light source in three quantities: radiance, luminance, and brightness. All colors are seen as variable combination of the three primaries in the RGB color model, which is usually used in representing and displaying images [10].

D. YIQ Color Model:

The YIQ color model is a widely supported standard in National Television Standards Commission (NTSC) color TV transmission. In this scheme, Y is proportional to the gamma-corrected luminance, which corresponds roughly with intensity, and I and Q jointly describe the chroma, which corresponds with hue and saturation, of a color image in the following relations with the RGB model [1]:

$$\begin{bmatrix} Y \\ I \\ Q \end{bmatrix} = \begin{bmatrix} 0.299 & 0.587 & 0.114 \\ 0.596 & -0.275 & -0.321 \\ 0.212 & -0.523 & 0.311 \end{bmatrix} \begin{bmatrix} R \\ G \\ B \end{bmatrix} \quad (1)$$

E. HSV Color Model:

Smith described a triangle-based HSV model in the following relations with the RGB model[1],[10]:

$$V = \frac{1}{3}(R + G + B) \quad (2)$$

$$S = 1 - \frac{3}{R+G+B} \min(R, G, B) \quad (3)$$

$$H = \begin{cases} \theta, & \text{if } B \leq G \\ 360^\circ - \theta, & \text{if } B > G \end{cases} \quad (4)$$

In which ,

$$\theta = \cos^{-1} \left\{ \frac{\frac{1}{2}[(R-G)+(R-B)]}{\sqrt{(R-G)(R-G)+(R-B)(G-B)}} \right\}$$

F. HCV Color Model:

The HCV model describes the dominant frequency, the amount of color, and luminance, respectively, in the following relations with the RGB model [1], [10]:

$$V = \frac{1}{3}(R + G + B) \quad (5)$$

$$H = \tan^{-1} \left[\frac{R-B}{\sqrt{3}(V-G)} \right] \quad (6)$$

$$C = \begin{cases} \frac{V-G}{\cos H}, & \text{if } |\cos H| > 0.2 \\ \frac{R-B}{\sqrt{3} \sin H}, & \text{if } |\cos H| \leq 0.2 \end{cases} \quad (7)$$

G. HSI Color Model:

The HSI model manipulates color images with the following transformation from the RGB model [1], [10]:

$$\begin{bmatrix} I \\ V_1 \\ V_2 \end{bmatrix} = \begin{bmatrix} \frac{1}{3} & \frac{1}{3} & \frac{1}{3} \\ -\sqrt{6} & -\sqrt{6} & \sqrt{6} \\ 6 & 6 & 3 \\ \frac{1}{\sqrt{6}} & \frac{-2}{\sqrt{6}} & 0 \end{bmatrix} \begin{bmatrix} R \\ G \\ B \end{bmatrix} \quad (8)$$

$$S = \sqrt{V_1^2 + V_2^2} \quad (9)$$

$$H = \tan^{-1}(V_2|V_1), \text{ where } V_1 \neq 0 \quad (10)$$

Note that hue and saturation taken together are called chromaticity and the brightness of a chromatic light embodies the achromatic notion of intensity.

H. YCbCr Color Model:

The YCbCr model is used in most video and image compression standards like JPEG, MPEG, and H2.63+ for the transmission of luma and chroma components coded in the integer range [0, 255]. It has the following relations with the RGB model[1],[10]:

$$\begin{bmatrix} Y \\ C_b \\ C_r \end{bmatrix} = \begin{bmatrix} 0.257 & 0.504 & 0.098 \\ -0.148 & -0.291 & 0.439 \\ 0.439 & -0.368 & -0.071 \end{bmatrix} \begin{bmatrix} R \\ G \\ B \end{bmatrix} + \begin{bmatrix} 16 \\ 128 \\ 128 \end{bmatrix} \quad (11)$$

For paper research, we are collected urban color aerial images which are shown in fig. 2. Image-1 is taken from [16], Image-2 to Image-4 is taken from different websites, Image-5 is captured by us, and Image-6 to Image-8 is taken from [17]. These images give appropriate results for our proposed work.



Fig. 2: Dataset of Color Aerial Images (A) Image-1, (B)Image-2, (C)Image-3, (D)Image-4, (E)Image-5, (F)Image-6, (G)Image-7, (H)Image-8, Respectively.

This paper is organized into the following sections. Section I gives an introductory part, basic information about shadow and shadow types, and also color models. Section II describes significant literature review on various shadow detection methods. Section III presents a detailed discussion on our proposed shadow detection work. In section IV, performance evaluation results are presented. Section V discusses experimental results of proposed work. Finally, Section VI concludes this paper.

II. LITERATURE REVIEW

Table 1 shows widely used shadow detection methods based on different approaches. Here a brief review of these methods is presented. Automatic property-based approach is applied by J.D.Tsai on invariant color models for detection and compensation of shadow regions with shape information preservation for solving problems in digital image mapping caused by cast shadows. This method is worked on color aerial images[1]. Illumination Assessment Method is implemented by J.M.Wang et.al., for detecting and removing shadows from foreground figures which have been extracted by background subtraction method from input image. This method is applied on outdoor images like traffic images [11]. In Adaboost classifiers in a co-training framework developed by Jie Zhao, Suhong Kong, and Guozun Men , a fraction of labeled data are demanded and then unlabeled data's is used to enhance categorical performance to detect shadows. This method is performed on video surveillance systems [12]. Gradient-based background subtraction method implemented by Muhammad Shoaib et.al. , is used for detecting cast shadows using contour like structures of objects which does not use any color information. This method is applied on video frame using contour of moving objects [13]. Harris detection algorithm developed by Zhiyong Ye, Yijian Pei ,Jihong Shi based on the neighboring point eliminating method which reduces the time of the detection, and makes the corners distributing more homogenous. This method is worked on urban material images such as buildings and trees [14]. Susan algorithm developed by Huang Si-ming, Liu Bing-han, Wang Wei-zhi is used for a method of moving shadow detection based on image edge detection to subtract the shadows occur in different circumstances. This method is applied on moving object images [15].

III. OUR PROPOSED WORK

In this section, we propose an extension of the work by J.D.Tsai[1] on chromaticity-based shadow detection approach to detect shadows from color aerial images. Fig. 3 shows different steps used to execute a Chromaticity-Based shadow detection approach. The RGB-based color aerial images are transformed into the various color spaces including YIQ, HSV, HIS, HCV, and YCbCr. The ratioing technique is applied to obtain ratio of intensity and hue component as ratio image, which is scaled to have pixels' values in [0, 255]. The (Q+1) / (I+1) ratio image shall enhance property of shadows with low luminance. Then post-processing methods are applied on ratio image, to further enhance the performance of shadow detection. Post-processing method contains three parts including histogram equalization, box filtering and thresholding using Otsu's

method. Histogram equalization method enhances the contrast of images by transforming the values in an intensity image, or the values in the color map of an indexed image. Box filter is applied on calculated histogram equalized image to alleviate the noise effect. Thresholding using Otsu's method is then applied over filtered image to automatically determine the threshold for segmenting the regions in shadow. Product of thresholded box filtered image and threshold ratio image is performed to remove non-shadow pixels from binary image which are appearing as shadow pixels. This step gives shadow pixels which are common in both the images being multiplied. At last, image close operation is applied on the thresholded image to preserve connectivity between shadowed pixels. Steps 1, 2 and 3 are taken from [1], and steps 4 and 5 are proposed by us. Overall operational steps of this approach for shadow detection are summarized below. It should be noted here that the original method[1] perform thresholding operation on ratio image directly to obtain shadow and non -shadow pixels.

SN.	Authors	Method	Highlights
1.	J.D.Tsai[1]	Automatic property-based approach in invariant color models	Decouple luminance and chromaticity to exploits properties of shadows.
2.	J.M. Wang, Y.C. Chung, C.L. Chang, and S.W. Chen[11]	Illumination Assessment Method	Presence of shadow in object is confirmed by illumination assessment method.
3.	Jie Zhao, Suhong Kong, and Guozun Men[12]	Adaboost Classifiers in a co-training Framework	Accuracy comparison is calculated by finding shadow detection rate and shadow discrimination accuracy.
4.	Muhammad Shoaib, Ralf Dragon, Jörn Oster Mann[13]	Gradient based background subtraction	Fixed threshold is set for T vertical and T horizontal boundary of object is extracted using mixture of Gaussians.
5.	Zhiyong Ye, Yijian Pei ,Jihong Shi[14]	Harris Algorithm	Neighboring point eliminating method used to detect from corner efficiently
6.	Huang Si-ming,Liu Bing-han, Wang Wei-zhi[15]	Susan Algorithm	Video highway data with avi format,edge is detected from Susan algorithm

Table 1: Summary of Various Shadow Detection Methods

- Step 1: Take a RGB color aerial image and separate each R, G, and B components of color image which ranges from 0 to 255.

- Step 2: Convert color space from RGB color model to YIQ color model using equations defined in various color spaces.

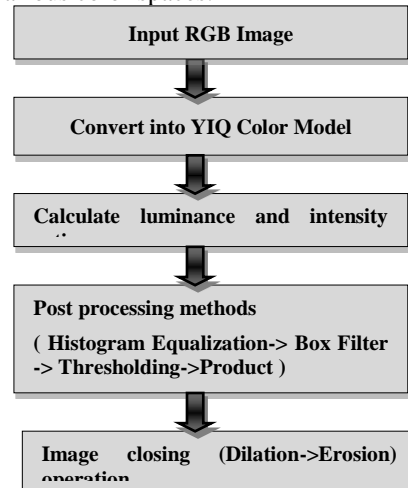


Fig. 3: Flowchart of the Proposed Work

- Step 3: Compute ratio maps by taking ratios of intensity and luminance (hue) components.
- Step 4: Apply post processing method on computed ratio image.
- Step 5: Apply image close operation on post processed resultant image.

IV. EXPERIMENTAL RESULTS

In this section, we present the experimental results with color aerial images using Chromaticity-Based shadow detection approach. As we are getting best results in YIQ space these results are only presented here. Our proposed method is applied on color aerial images. It gives better results than existing shadow detection techniques as shown in fig. 4 and fig. 5, respectively. They shows original color aerial images, computed ratio image, resultant post processing image and finally, shadow detected image, respectively.

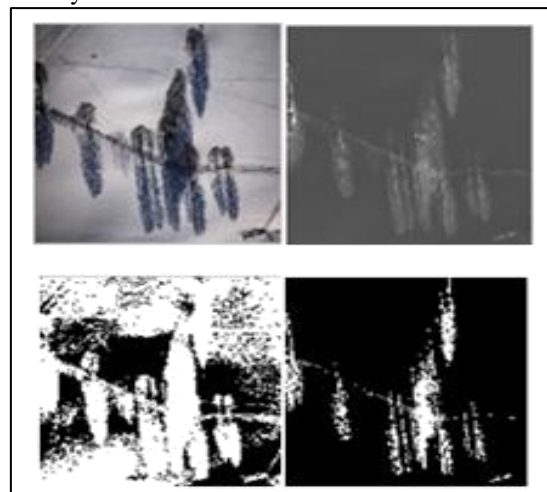


Fig. 4: Detection of Shadows (Represented As White Pixels) According To Proposed Work On Image-2 (A) Original Image (B) Ratio Image (C) Post Processing Image (D) Image Obtained After Image Close Operation

Shadow detected image is a binary image in which 0 represents non-shadow pixels i.e. black pixels and 1 represents shadow pixels i.e. white pixels. Performance of

proposed technique is better than existing shadow detection techniques.

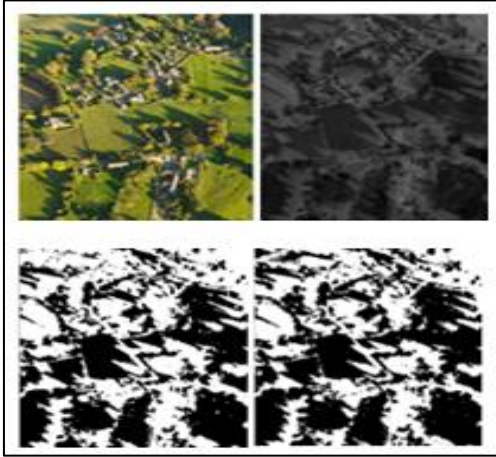


Fig. 5: Detection of Shadows According To Proposed Work on Image-4 (A) Original Image (B) Ratio Image (C) Post Processing Image (D) Image Obtained After Image Close Operation

Comparing the result obtained using our approach as shown in Fig. 6 (d) with the existing approach as shown in Fig. 6 (c), it is observed that there is misclassification of non-shadow represented by circles with existing approach which is eliminated by using the proposed approach.

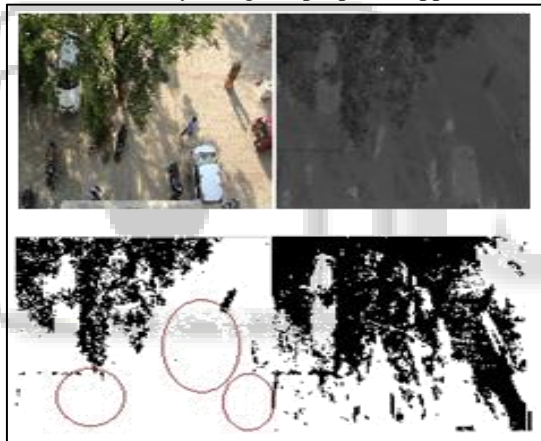


Fig. 6: Comparative Results For Image-5 (A) Original Image (B) Ratio Image (C) Shadow Detected Image Using Original Approach (D) Shadow Detected Image Using Proposed Approach

V. PERFORMANCE EVALUATION

The performance evaluation metrics of shadow detection accuracy assessment is applied on Image-6 and Image-7 as shown in fig. 7 and fig. 8, respectively, at pixel level which contains three types of accuracy are described as follows.

A. Producer's Accuracies:

The producer's accuracy is computed for correctness of algorithm in terms η_s and η_n , and they are defined as

$$\eta_s = \frac{TP}{TP + FN}$$

$$\eta_n = \frac{TP}{TN + FP}$$

where true positive (TP) denotes the number of true shadow pixels (i.e. white pixels) which are identified correctly; false negative (FN) denotes the number of true

shadow pixels which are identified as nonshadow pixels; false positive (FP) denotes the number of nonshadow pixels which are identified as true shadow pixels; and true negative (TN) is the number of nonshadow pixels (i.e. black pixels) which are identified correctly. The parameter η_s denotes the ratio of the number of correctly detected true shadow pixels over that of total true shadow pixels and, η_n denotes the ratio of number of correctly detected true non-shadow pixels over that of total true non-shadow[1],[3].



Fig. 7: Performance Evaluation Results for Image-6 (A) Original Image (B) Shadow Ground Truth (C) Shadow Detected Using the Proposed Algorithm



Fig. 8: Performance Evaluation Results For Image-7(A) Original Image (B) Shadow Ground Truth (C) Shadow Detected Using The Proposed Algorithm.

B. User's Accuracies:

The User's accuracy used to compute precision of algorithm which contains two parameters ps and as follows

$$ps = \frac{TN}{TN + FN}$$

$$pn = \frac{TP}{TP + FP}$$

The parameter ps (pn) denotes the ratio of the number of correctly detected true shadow (non-shadow) pixels over that of the total detected true shadow (non-shadow) pixels[1],[3].

C. Overall Accuracy:

Combining the accuracies of the user and the producer, the third type of accuracy τ defined as follows can be used to evaluate the correctness percentage [2] of the algorithm:

$$\tau = \frac{TP + TN}{TP + TN + FP + FN}$$

Where $TP + TN$ denotes the number of correctly detected true shadow and non-shadow pixels; $TP + TN + FP + FN$ is equal to the number of total pixels in the image.

Method	Producer's accuracies		User's accuracies		Overall accuracy
	Shadow η_s (%)	Nonshadow η_n (%)	Shadow ps (%)	Nonshadow pn (%)	
Proposed	60.8682	60.2410	99.7515	0.5837	60.8658
Tsai's	59.2837	63.9535	99.7642	0.6324	59.2982

Table 2: Shadow Detection Performance Evaluation for Image-6

Using these accuracy equations, we measure performance evaluation metrics of our proposed work for YIQ color space which gives better results than existing work shown in TABLE 2 and TABLE 3, respectively.

Method	Producer's accuracies		User's accuracies		Overall accuracy
	Shadow $\Pi_s(\%)$	Nonshadow $\Pi_n(\%)$	Shadow $\Pi_s(\%)$	Nonshadow $\Pi_p(\%)$	
Proposed	84.7493	69.9029	99.9441	0.7163	84.7260
Tsai's	81.0770	43.4783	99.9755	0.0806	81.0638

Table 3: Shadow Detection Performance Evaluation For Image-7

VI. CONCLUSION AND FUTURE SCOPE

In this work we have implemented existing automatic property-based shadow detection technique developed by Victor J. D. Tsai. The technique is applied in few color spaces that decouple luminance and chromaticity, including HSI, HSV, HCV, YIQ, and YCbCr models. We have extended this approach by using proposed post processing methods. Our approach gives best results with YIQ color space. The comparison of results obtained by our approach in YIQ color space, with the existing technique is presented. The performance evaluation results presented in Table 2 and 3 indicates the improvement of the producer's and user's accuracies with this post processing approach. In future, we will work on shadows removal algorithms in these color spaces using our approach.

REFERENCES

[1] J.D.Tsai, "A comparative study on shadow compensation of color aerial images in invariant color models," IEEE Trans. Geosci. Remote Sens., vol. 44, no. 6, pp. 1661–1671, Jun. 2006.

[2] Wenxuan Shi* and Jie Li, "Shadow detection in color aerial images based on HSI space and color attenuation relationship", Shi and Li EURASIP Journal on Advances in Signal Processing 2012. <http://asp.eurasipjournals.com/content/2012/1/141>.

[3] Kuo-Liang Chung, Yi-Ru Lin, and Yong-Huai Huang, "Efficient Shadow Detection of Color Aerial Images Based on Successive Thresholding Scheme", IEEE transactions on geoscience and remote sensing, vol. 47, no. 2, february 2009.

[4] D. Sunil Kumar1, M.Gargi2, "An Approach in Shadow Detection and Reconstruction of Images", International Journal of Application or Innovation in Engineering & Management (IJAIEM), Volume 2, Issue 7, July 2013 ISSN 2319 - 4847.

[5] Maryam Basij, Payman Moallem, Mohammadreza Yazdchi, Shahed Mohammadi, "Automatic Shadow Detection in Intra Vascular Ultrasound Images Using Adaptive Thresholding", 2012 IEEE International Conference on Systems, Man, and Cybernetics October 14-17, 2012, COEX, Seoul, Korea.

[6] Sooho Park and Sejoon Lim, "Fast Shadow Detection for Urban Autonomous Driving Applications", 2009 IEEE/RSJ International Conference on Intelligent Robots and Systems October 11-15, 2009 St. Louis, USA.

[7] Luca Lorenzi, Farid Melgani, Grégoire Mercier, "A Complete Processing Chain for Shadow Detection and Reconstruction in VHR Images", IEEE transactions on geoscience and remote sensing, VOL. 50, NO. 9, SEPTEMBER 2012.

[8] Hakima Asaidi a., Abdellah Aarab, Mohamed Bellouki, "Shadow Detection Approach Combining Spectral and Geometrical Properties", 2012 IEEE.

[9] AmirReza SHAHTAHMASSEBI1, YANG Ning1, WANG Ke1, Nathan MOORE2, SHEN Zhangquan1, "Review of Shadow Detection and De-shadowing Methods in Remote Sensing", Chin. Geogra. Sci. 2013 Vol. 23 No. 4 pp. 403–420 Springer Science Press doi: 10.1007/s11769-013-0613-x.

[10] R.C. Gonzalez and R.E.Woods, Digital Image Processing, Reading, MA: Addison-Wesley, 1992.

[11] J.M. Wang, Y.C. Chung, C.L. Changt, and S.W. Chen, "Shadow Detection and Removal for Traffic Images", Proceedings of the 2004 IEEE International Conference on Networking, Sensing & Control Taipei, Taiwan, March 21-23, 2004.

[12] Jie Zhao, Suhong Kong, and Guozun Men, "Shadow Detection Based on Adaboost Classifiers in a Co-training Framework", 2011 IEEE.

[13] Muhammad Shoab, Ralf Dragon, Jörn Ostermann, "shadow detection for moving humans using gradient-based Background subtraction", 2009 IEEE.

[14] Zhiyong Ye, Yijian Pei, Jihong Shi, "An Improved Algorithm for Harris Corner Detection", 2009 IEEE.

[15] Huang Si-ming, Liu Bing-han, Wang Wei-zhi, "Moving shadow detection based on Susan algorithm", 2011 IEEE.

[16] Jiahang Liu, Tao Fang, and Deren Li, "Shadow Detection in Remotely Sensed Images Based on Self-Adaptive Feature Selection", IEEE TRANSACTIONS ON GEOSCIENCE AND REMOTE SENSING, VOL. 49, NO. 12, DECEMBER 2011.

[17] RuiqiGuo, Qieyun Dai, and Derek Hoiem, "Paired Regions for Shadow Detection and Removal", IEEE TRANSACTIONS ON PATTERN ANALYSIS AND MACHINE INTELLIGENCE, VOL. 35, NO. 12, DECEMBER 2013.